

1 **Aqueous and non-aqueous microchip electrophoresis with on-chip electrospray ionization**
2 **mass spectrometry on replica-molded thiol-ene microfluidic devices**

3
4 Sari Tähkä^a, Ashkan Bonabi^a, Ville Jokinen^b and Tiina Sikanen^{a*}

5
6
7 ^aFaculty of Pharmacy, Drug Research Programme, University of Helsinki, Viikinkaari 5E, FI-00014
8 University of Helsinki, Helsinki, Finland; Email: sari.tahka@helsinki.fi, ashkan.bonabi@helsinki.fi,
9 tiina.sikanen@helsinki.fi

10 ^bDepartment of Materials Science and Engineering, School of Chemical Technology, Aalto
11 University, Tietotie 3, FI-00076 Aalto, Espoo, Finland; Email: ville.p.jokinen@helsinki.fi

12
13 ***Corresponding author**

14 Dr. Tiina Sikanen, Division of Pharmaceutical Chemistry and Technology, Faculty of Pharmacy,
15 P.O. Box 56 (Viikinkaari 5E), FI-00014 University of Helsinki, Finland; E-mail:
16 tiina.sikanen@helsinki.fi; Tel. +358-2941-59173

17

18 **ABSTRACT**

19

20 This work describes aqueous and non-aqueous capillary electrophoresis on thiol-ene-based
21 microfluidic separation devices that feature fully integrated and sharp electrospray ionization (ESI)
22 emitters. The chip fabrication is based on simple and low-cost replica-molding of thiol-ene polymers
23 under standard laboratory conditions. The mechanical rigidity and the stability of the materials against
24 organic solvents, acids and bases could be tuned by adjusting the respective stoichiometric ratio of
25 the thiol and allyl (“ene”) monomers, which allowed us to carry out electrophoresis separation in both
26 aqueous and non-aqueous (methanol- and ethanol-based) background electrolytes. The stability of
27 the ESI signal was generally $\leq 10\%$ RSD for all emitters. The respective migration time repeatabilities
28 in aqueous and non-aqueous background electrolytes were below 3 and 14% RSD (n= 4-6, with
29 internal standard). The analytical performance of the developed thiol-ene microdevices was shown in
30 mass spectrometry (MS) based analysis of peptides, proteins, and small molecules. The theoretical
31 plate numbers were the highest ($1.2\text{-}2.4 \times 10^4 \text{ m}^{-1}$) in ethanol-based background electrolytes. The
32 ionization efficiency also increased under non-aqueous conditions compared to aqueous background
33 electrolytes. The results show that replica-molding of thiol-enes is a feasible approach for producing
34 ESI microdevices that perform in a stable manner in both aqueous and non-aqueous electrophoresis.

35

36 **Keywords:** Microchip electrophoresis, Non-aqueous capillary electrophoresis, Electrospray
37 ionization, Mass spectrometry, Replica-molding, Thiol-enes

38 1. INTRODUCTION

39 Microchip capillary electrophoresis (MCE) is the gold standard of microfluidic separation systems.
40 MCE in combination with electrospray ionization mass spectrometry (ESI-MS) is a promising tool
41 for modern bioanalysis, especially in proteomics and metabolomics.[1] Although numerous
42 approaches for interfacing separation microdevices with MS *via* ESI exist, the implementation of on-
43 chip ESI emitters as an integral part of the separation chip is feasible for only a few microfabrication
44 methods and materials. One important limitation is that fabrication typically requires expensive
45 cleanroom instrumentation.[2, 3] Integration of a sharp-pointed, on-chip ESI emitter directly with the
46 separation microchannel outlet eliminates the dead volume at the ESI interface and the need for
47 manual post-processing required to attach off-chip emitters. In addition, a sharp-pointed tip reduces
48 sample spreading at the channel outlet and facilitates producing the small Taylor cone that is required
49 for efficient ionization (small droplet size) and stable spraying. Integrated MCE devices with on-chip
50 emitters have been made from glass by manual pulling the ESI emitter [4], by sawing a sharp corner
51 at the microchannel outlet [5, 6] and by isotropic etching [7] techniques. Silicon [8] or silicon-glass
52 hybrid materials [9] have also been used for fabricating on-chip ESI emitters onto chromatographic
53 separation chips. The semiconductive properties of silicon, however, render it unfeasible for
54 electrophoresis applications.

55
56 The lowest-cost approach for fabrication of sharp-pointed ESI emitters appears to be achieved *via*
57 polymer microfabrication. Electrophoresis separation chips with sharp-pointed, on-chip ESI emitters
58 have been implemented on SU-8 by standard photolithography [10], on organically modified
59 ceramics by sawing [11], on polycarbonate by laser micromachining [12] and on cyclo-olefins by hot
60 embossing [13]. However, high-precision fabrication and bonding of the above mentioned materials
61 require expensive instrumentation or special facilities, such as a cleanroom environment. This
62 constraint inevitably hinders the wider adoption of the microchip technology to routine laboratory

63 analyses. Thus, non-cleanroom polymer processing methods, such as the replication of polydimethyl
64 siloxane (PDMS) [14], have also been introduced as an approach to achieve the low-cost fabrication
65 of on-chip emitters. In addition to its straightforward replication, PDMS also allows for the easy
66 sealing of microchannel by adhesive bonding of two cross-linked layers. The drawbacks to PDMS,
67 however, is that it is susceptible to swelling and severe monomer leaching upon exposure to organic
68 solvents [15, 16] and it also undergoes significant nonspecific adsorption of biomolecules unless the
69 surface is physically or chemically treated prior to use [17]. Moreover, the elasticity of PDMS
70 prevents fabrication of very thin layers, which is often desired as a prerequisite to reproduce three-
71 dimensionally sharp ESI emitters.

72

73 We describe a new, low-cost method for the fabrication of MCE-ESI microdevices with fully
74 integrated, thin and sharp on-chip ESI emitters using the approach of replica-molding of thiol-ene
75 polymers. In addition, thiol-enes enable adhesive bonding similar to that of PDMS, but show much
76 better stability against organic solvents. The mechanical stiffness and rigidity of thiol-enes can also
77 be tuned by altering the respective quantities of the thiol and allyl (“ene”) monomers in the bulk
78 material.[18] The use of off-stoichiometric monomer ratios results in excess of free thiol or allyl
79 functional groups on the polymer surface [19-21] which have been exploited for numerous
80 biofunctionalizations [22-25] and for aqueous MCE in combination with fluorescence detection. [19,
81 22, 26] Thiol-ene channels generally maintain high cathodic electroosmotic flow over a wide pH
82 range (pH 3-12) [19, 22] and show little nonspecific adsorption of peptides in native, allyl-rich
83 microchannel walls. [19] Polyacrylate copolymer coatings can be used to eliminate protein adsorption
84 in thiol-rich microchannels. [22]

85 Thanks to their inherent good stability against organic solvents, thiol-enes as chip fabrication
86 materials also provide greater flexibility in terms of analytical method development than most other
87 microfabrication polymers. In this study, we exploit the good solvent compatibility to carry out

88 microchip electrophoresis in non-aqueous conditions. The study demonstrates how the selection
89 between aqueous and non-aqueous background electrolyte affects not only the separation efficiency
90 and selectivity, but also sensitivity and repeatability. Thus far only a very few on-chip NACE
91 applications (in combination with any detector) have been reported. [27-30] The fabrication of sharp,
92 on-chip emitters that use solvent-compatible fabrication materials (such as glass) is challenging [2]
93 and thus the combination of microchip NACE and on-chip ESI is less common than its aqueous-phase
94 counterpart despite the inherently good technical compatibility between NACE and ESI-MS. The
95 replica-molding of thiol-enes presented in this work achieves fabrication of an integrated, sharp
96 emitter at low-cost and the produced MCE-ESI devices show good analytical performance in both
97 aqueous and non-aqueous electrophoresis.

98

99 **2. EXPERIMENTAL**

100 **2.1. Materials and Reagents**

101 Acetic acid, methanol, ethanol, propanol and acetonitrile were purchased from Sigma-Aldrich
102 (Steinheim, Germany). Ammonium acetate and hydrochloric acid were purchased from Riedel-de
103 Haën (Seelze, Germany). Formic acid was purchased from Merck Millipore (Darmstadt, Germany).
104 Angiotensin I human acetate salt hydrate ($\geq 90\%$), angiotensin III ($\geq 98\%$) and cytochrome c from
105 bovine heart (12327 Da $\geq 95\%$) were from Sigma-Aldrich. Angiotensin II acetate salt (96.2%) was
106 from Bachem (Bubendorf, Switzerland). Verapamil hydrochloride was from ICN Biomedicals
107 (Aurora, OH). Stock solutions of peptides (each 1 mg/mL in milli-Q water), cytochrome c (5 mg/mL
108 in water) and verapamil (1 mM in MeOH) were diluted before analysis in respective solvents. All
109 reagents and solvents used were of HPLC or LC-MS grade ($\geq 99.0\%$) unless otherwise stated. Water
110 was purified with a Milli-Q water purification system (Millipore, Molsheim, France).

111

112 Trimethylolpropanetri(3-mercaptopropionate) ('trithiol') ($\geq 95.0\%$), pentaerythritoltetrakis(3-
113 mercaptopropionate) ('tetrathiol') ($\geq 95.0\%$) and 1,3,5-triallyl-1,3,5-triazine-2,4,6(1H,3H,5H)-trione
114 ('triene') ($\geq 98.0\%$) were purchased from Sigma-Aldrich (Saint Louis, MO, USA). Poly(dimethyl
115 siloxane) (PDMS) was prepared from Sylgard 184 base elastomer and curing agent (Down Corning
116 Corporation, Midland, MI, USA). SU-8 negative photoresist (Microchem Corporation, Newton, MA,
117 USA) were purchased from Micro Resist Technologies GmbH (Darmstadt, Germany).

118

119 **2.2. Microchip fabrication**

120 Thiol-ene chips were fabricated by mixing commercially available trithiol or tetrathiol monomers
121 with triallyl ("triene") monomer in stoichiometric or off-stoichiometric ratios (50 mol-% excess of
122 allyls, trithiols or tetrathiols). No photoinitiator or other additives were used during the thiol-ene
123 crosslinking process. First, a PDMS negative mold was prepared from a 4-inch SU-8 master. This
124 wafer-scale mold featured 12 parallel MCE-ESI units, each incorporating the separation
125 microchannel with an integrated electrospray emitter.. The thiol and allyl monomers were mixed and
126 poured onto the PDMS mold (Figure 1A-D). The thiol-ene mixture was cured without any cover plate
127 or photomask by exposing it to UV from a Dymax 5000-EC Series UV flood exposure lamp (Dymax
128 Corporation, Torrington, CT, USA, nominal power of 225 mW/cm^2). The UV exposure times were
129 chosen based on our earlier study [19] and were 10 min for all thiol-ene compositions. The bottom
130 layer of the thiol-ene chip, featuring only the outer edges of the chip, was prepared in a similar manner
131 and laminated against the microchannel layer. The thiol-ene layers were preheated to 70°C before
132 lamination to gently soften the polymer and thus obtain uniform sealing between the layers. The
133 lamination was done under a stereomicroscope to ensure precise alignment of the two thiol-ene layers
134 at the emitter area. Last, the bonding was completed by additional UV exposure of 5 min similar to
135 that described in earlier work [19, 26].

136

137 The masters for the PDMS molds were made from SU-8 negative photoresist under cleanroom
138 conditions and were separately prepared for the microchannel and the bottom layers (Figure 1A). The
139 microfabrication protocols for the SU-8 master and the PDMS mold are described in detail in the
140 Supplement material.

141

142 The fabricated microchips featured a 20-mm-long separation channel (effective length) that
143 incorporated a simple cross injection channel and was intersected by a 10-mm-long makeup liquid
144 channel just behind the emitter tip (Figure 1E). The cross-section dimensions of the separation
145 channel were $50\ \mu\text{m} \times 50\ \mu\text{m}$ (w×h), of the injection channel $30\ \mu\text{m} \times 50\ \mu\text{m}$ (w×h) and of the makeup
146 liquid channel $200\ \mu\text{m} \times 50\ \mu\text{m}$ (w×h). The inlets were 1 mm in diameter and the thickness of the
147 emitter tip was approximately $200\ \mu\text{m}$ (Figure 1F)

148

149 **2.3. Solvent exposure tests**

150 The stabilities of the stoichiometric and various altered off-stoichiometric thiol-ene compositions
151 were tested against selected organic solvents (methanol, ethanol, propanol and acetonitrile), acids
152 (10 % formic acid, 10 % acetic acid, 2 M hydrochloric acid) and bases (10% ammonium hydroxide)
153 commonly used in MS applications. Thiol-ene slabs (thickness 0.5 mm, $A=1\ \text{cm}^2$) that had been cured
154 for 10 min were used as test pieces. The pieces were immersed in 1 mL of each solvent for 1 h or for
155 4 days after which they were visually monitored for any mechanical damage, e.g., swelling,
156 degradation, or defects on the surface.

157

158 **2.4. Microchip electrophoresis-electrospray ionization mass spectrometry**

159 The thiol-ene microchips were coupled to an Agilent 6330 iontrap mass spectrometer (Agilent
160 Technologies, Santa Clara, CA) equipped with a modified nanospray frame (Proxeon Biosystems,
161 Odense, Denmark), which featured an xyz aligning stage and a CCD camera (Figure S1). The ion

162 trap was operated in positive ion mode with a capillary voltage set at -1200 or -1500 V and end plate
163 offset at -500 V. Nitrogen produced from compressed air by a Parker nitrogen generator (Cleveland,
164 OH) was used as the drying gas with a flow rate of 4.0 L/min at 70°C. The MS data were acquired by
165 averaging two cycles over a mass range of m/z 100–2200 with maximum accumulation time of 200
166 ms. Data Analysis 3.4 was used for data acquisition and processing.

167 Before use, thin PDMS sheets with 2 mm inlet holes were attached on top of the inlets to increase the
168 sample volume and to limit spreading of the sample and buffer aliquots over the chip surface. Since
169 PDMS was only used as passive support structures, no PMDS monomer leaching to the MS was
170 observed. An external high voltage power supply (Micralyne, Edmonton, AB) was used to apply the
171 ESI and the separation voltages through platinum wires placed in the microchannel inlets. The
172 samples were introduced through a simple injection cross by applying an injection voltage of +800 V
173 to the sample inlet (SI) and grounding the sample outlet (SO) for 20.0 s. The nominal injected sample
174 volume ($V=75$ pL) was defined by the injection cross geometry, which was $30\ \mu\text{m}\times 50\ \mu\text{m}\times 50\ \mu\text{m}$
175 ($w\times L\times h$). The make-up liquid inlet (MLI) was floating during injection. The MCE separation was
176 performed by applying a separation voltage (typically 4900-4700V) to the buffer inlet (BI) and
177 antileakage voltages (typically 4500-4000V) to the SI and SO. The ESI voltage, which also served as
178 the counter voltage for the MCE separation was applied to the MLI and was between 2000 and 3500
179 V (see Supplementary material Figure S1). The separation current was typically between 30–40 μA ,
180 and the electrospray current less than 200 nA. Thanks to the laminarity of flows, the make-up liquid
181 did not much dilute the sample flow prior to ESI-MS. The excess current from the separation channel
182 was grounded through a 50 $\text{M}\Omega$ resistor coupled in parallel with the ES voltage supply. The distance
183 between the tip and the MS orifice was typically between 5 and 10 mm.

184

185

186 **3. RESULTS AND DISCUSSION**

187 **3.1. Fabrication and material stability aspects**

188 This work describes simple and low-cost fabrication of microfluidic electrophoresis chips with fully
189 integrated on-chip emitter tips *via* UV replication of thiol-ene polymers under standard laboratory
190 conditions. We used PDMS (negative) molds replicated from SU-8 masters as the templates for
191 replica-molding of thiol-enes. Each SU-8 master (featuring 12 parallel MCE-ESI units) could be re-
192 used for PDMS molding for at least 5-10 times and each PDMS mold (also featuring 12 parallel
193 MCE-ESI units) for thiol-ene replication for at least 5 times. This totals minimum of 300 thiol-ene
194 MCE-ESI chips reproduced out of a single SU-8 master. Thus, the materials cost of a single thiol-ene
195 chip becomes very low. Also the infrastructure needed for thiol-ene replication included only low-
196 cost, standard equipment such as flood exposure lamp and oven. Only the fabrication of the SU-8
197 master was carried out using established cleanroom techniques (see Supplementary material) and thus,
198 the cost of the fabrication and the need for cleanroom processing were significantly reduced compared
199 to fully cleanroom-microfabricated glass [4-7] or SU-8 [10] electrospray microchips, for example.
200 Therefore the ease of replica-molding and bonding of thiol-enes significantly promotes the use of
201 microchip based techniques in routine MS analyses by providing new technical solutions to chip
202 fabrication that are accessible to all. The only critical step of the thiol-ene chip fabrication was the
203 bonding of the two cured layers together with high precision in alignment at the emitter tip. However,
204 if misalignment occurred, it was possible to re-do the bonding step before the bond was finalized by
205 additional UV curing. Since the PDMS molding and thiol-ene replication steps were carried out in a
206 laminar flow hood, the particles in the regular laboratory air mainly landed on the chip surface and
207 had thus negligible influence on the device performance (e.g., the flow rate or the migration of the
208 analytes inside the microchannel).

209

210 Only PDMS of the other commonly used polymer materials allows an equally straightforward
211 adhesive bonding as that of thiol-enes, but the elasticity of PDMS prevents the replication of thin
212 emitters. Instead, the good mechanical strength and rigidity of the thiol-ene compositions used in this
213 study allowed the fabrication of relatively thin microchips (ca. 200 μm at the tip, Figure 1F), which
214 enabled the reproduction of three-dimensionally sharp tips. Comparison of the tensile strengths of the
215 different thiol-ene formulations (see Supplementary material Figure S3) indicates how the
216 mechanical properties of crosslinked thiol-enes are affected by both the monomer ratio and the
217 selection of the precursor monomers (trithiol vs. tetrathiol). For example, off-stoichiometric
218 compositions comprising excess quantities of trithiol monomers formed relatively elastic structures,
219 which complicated thiol-ene-to-thiol-ene bonding and also hindered the fabrication of rigid and sharp
220 emitters. However, replacement of the trithiol monomer with tetrathiol enabled the fabrication of
221 sufficiently rigid MCE-ESI microchips while still having thiol-rich surfaces. Stoichiometric and allyl-
222 rich compositions also resulted in sufficiently rigid structures.

223

224 Apart from elasticity, good chemical stability is essential for obtaining reproducible analytical
225 performance. Good compatibility with aliphatic and aromatic organic solvents has been reported for
226 thiol-ene polymers. [31-33] However, limited information exists about the stability against acids and
227 bases that are commonly used in MS applications. The compatibilities of the different thiol-ene
228 compositions used in this study with the selected organic solvents, acids and bases were thus
229 determined and are summarized in the Supplementary material (Table S1) together with photographs
230 and light microscope images of thiol-ene surfaces exposed to selected solvents (Figure S4). Briefly,
231 all compositions tested showed good resistance to methanol, ethanol, and propanol during short-term
232 exposure (1 h), whereas acetonitrile caused cracking and fragmentation of all the thiol-ene
233 compositions. The thiol-rich (50 mol-%) composition prepared from trithiol underwent cracking upon
234 long-term methanol exposure, but all other compositions, including the tetrathiol-rich (50 mol-%

235 excess) composition, tolerated the tested alcohols for extended periods of time (up to 4 days) without
236 incurring any clear defects. Similarly, none of the acid or base solutions had any influence on the
237 stoichiometric, allyl-rich (50 mol-%) or tetrathiol-rich (50 mol-%) composed devices during short or
238 long-term exposure. Only the trithiol-rich composition underwent cracking during prolonged
239 exposure (4 days) to acetic acid. Clearly, the lower crosslinking density of the trithiol-rich thiol-ene
240 composition causes not only less stiffness [21], but also makes the composition more vulnerable to
241 degradation upon exposure to organic solvents, acids and bases. Again, replacing the trithiol
242 monomer with tetrathiol resulted in greater stiffness and improved solvent compatibility.

243

244 **3.2. Electrospray performance**

245 Monomer leaching (due to incomplete crosslinking) from the bulk polymer to the MS is a well-known
246 drawback for many polymer based electrospray chips. Such leaching has detrimental effects upon the
247 analytes' ionization efficiency and upon the quality of the MS spectra obtained. PDMS in particular
248 has poor material stability regarding to leaching, although it has been reported that the cross-linking
249 density (i.e., the curing time) plays an important role in reducing the monomer leaching from PDMS
250 devices. [16, 34] Thiol-enes, on the other hand, are often used for chip fabrication in off-
251 stoichiometric ratios in order to achieve the desired mechanical properties or surface chemistry (thiol-
252 or allyl rich surfaces) that facilitates further biofunctionalization reactions.[21-26] To examine if the
253 use of off-stoichiometric formulations cause leaching of the excess monomers to the MS, we
254 compared the ESI-MS background spectra of microchips fabricated from each of the four different
255 thiol-ene formulations, each of which had two different curing times (10 or 20 min). The MS
256 background spectra were recorded by electrospraying sample solutions containing an
257 antihypertensive drug, verapamil (m/z 455.4), as an internal reference of the ESI stability.

258

259 As expected, allyl (m/z 250.1), trithiol (m/z 399.1) and tetrathiol (m/z 489.0) monomers leached out
260 of the chip whenever they were used in excess in the bulk composition and were observed as
261 protonated ions at their respective m/z (Figure 2A, C and D). The extension of the curing time from
262 10 to 20 min did not significantly reduce the background interference that originated from the off-
263 stoichiometric compositions. Despite this, the background interference was relatively low and could
264 be effectively eliminated by rinsing the channels prior to experiments. Most importantly, the
265 microchips that had been prepared from stoichiometric thiol-ene provided good quality spectra with
266 no traces of uncured monomers even without rinsing before the experiments (Figure 2B).

267

268 The performance of the ESI emitters prepared from different thiol-ene compositions was also
269 examined by comparing the total ion current (TIC) and the extracted ion current (EIC) stabilities of
270 the test compound verapamil. The TIC stabilities of the ESI emitters that had been fabricated from
271 allyl-rich (50 mol-%), tetrathiol-rich (50 mol-%) or stoichiometric thiol-ene compositions typically
272 ranged between 4.6 and 7.0% RSD, whereas their EIC stabilities ranged between 6.1 and 8.9% RSD
273 (n=3 chips, over 2 min range). As stated above, the fabrication of thin emitter tips from the trithiol-
274 rich composition (50 mol-% excess) was difficult due to its high elasticity and lack of rigidity. Thus,
275 the trithiol-rich emitter tips bent during electrospray and stable ion current was hardly obtained
276 (Figure 2C).

277

278 Apart from the trithiol-rich emitters, stable ion current could be easily maintained for as long as 20
279 min with an overall stability of 10.4% RSD (Figure S2). The chip-to-chip repeatability of the average
280 total ion current obtained by direct infusion was 13.3 % (n=4 chips). Each chip could also be re-used
281 for multiple analyses for several days. In addition to small molecule analysis, the feasibility of the
282 thiol-ene emitters was shown for direct infusion of a protein sample (cytochrome c), which showed
283 no interfering background originating from thiol-enes even in the high m/z range and thus good

284 accuracy (12230.5 ± 0.5 Da, 0.004% accuracy) in terms of molecular weight determination (Figure
285 3A).

286

287 These results suggest a high level of feasibility of thiol-ene replica-molding for fabrication of sharp
288 ESI emitters producing stable electrospray. The performance of the developed thiol-ene emitters in
289 ESI-MS was generally similar to those of the previously reported state-of-the-art microfabricated
290 emitters made of, e.g., glass, SU-8, or organically modified ceramics (see Table S3 for details). [2]
291 However, in comparison to other common microfabrication materials, the thiol-ene chemistry
292 provides greater flexibility in terms of chip fabrication (mechanical stiffness/rigidity and possibility
293 for low-cost, non-cleanroom replication), improved material stability against alcohols (methanol,
294 ethanol and propanol tested in this study), and more opportunities to tune both the surface chemistry
295 and the bulk properties toward the desired applications, without affecting the ESI-MS performance
296 much. Finally, the feasibility of the design to MCE-ESI-MS analysis was examined with help of
297 excitatory neuropeptides, Orexin A and B (Figure 3B). These peptides, however, suffered from
298 nonspecific adsorption to the native thiol-ene surface (as evidenced by pronounced peak tailing) and
299 did not resolve from each other within the short separation distance used (effective separation length
300 20 mm), leaving a place for further separation method development.

301

302 **3.3. Capillary zone electrophoresis in aqueous and non-aqueous conditions**

303 In addition to ESI-MS, we addressed the separation performance of the thiol-ene devices in both
304 aqueous and non-aqueous electrophoresis. For this purpose, we chose angiotensin II, a peptide
305 hormone that affects vasoconstriction, and its biologically inactive precursor, angiotensin I, the ratio
306 of which is an important biological indicator of angiotensin-converting enzyme (ACE) activity. The
307 MCE-ESI-MS analysis of the two angiotensins in aqueous conditions is shown in Figure 4A. The
308 repeatability of the migration time for angiotensin I and II were 4.6 and 4.7% RSD (2.7 and 2.4%

309 with angiotensin III as the internal standard, $n=4-5$) and the theoretical plate numbers 0.77×10^4 and
310 $0.80 \times 10^4 \text{ m}^{-1}$, respectively. However, even if MS detection could distinguish between the two forms
311 based on their different m/z values, the two peptides did not resolve electrophoretically from each
312 other within the short separation distance of 20 mm (similar to the Orexin peptides). Although these
313 peptides can be separated electrophoretically [35], the resolution poses a challenge because of the
314 similarities of their pI values (i.e. 7.70 v.s. 7.54 [36]) and their electrophoretic mobilities in aqueous
315 buffers. [37] In non-aqueous background electrolytes, the change in the solvents' ϵ/η ratio (see
316 Supplementary material, Table S2) may have a favorable effect on the resolving power and separation
317 selectivity. Moreover, the electroosmotic flow of non-aqueous background electrolytes is typically
318 slower than that of aqueous electrolytes leaving more time for the compounds to resolve
319 electrophoretically even in relatively short separation channels.

320

321

322 Therefore, we chose to study the possibility to use methanol and ethanol based, non-aqueous
323 background electrolytes to improve the resolving power of the two angiotensins,. Acetonitrile is
324 another commonly used solvent in NACE, but it was excluded due to its poor compatibility with
325 thiol-enes as described in the Supplementary material (Table S1). The analytical performance of on-
326 chip NACE in the analyses of the angiotensin peptides was compared to that obtained under aqueous
327 conditions using angiotensin III as the internal standard. As expected, the apparent mobilities of the
328 angiotensins decreased from ca. $4.5 \times 10^{-4} \text{ cm}^2 \text{ s}^{-1} \text{ V}^{-1}$ in aqueous electrolytes to $1.2 \times 10^{-4} \text{ cm}^2 \text{ s}^{-1} \text{ V}^{-1}$ in
329 organic background electrolytes (Figure 4F) as a result of the decreased EOF and the change in the
330 ϵ/η ratio of the solvent and thus decrease in electrophoretic mobilities of the two peptides. On the
331 basis of the comparison of the migration times between aqueous and methanol solutions (on the
332 average between 20 and 30 s) and ethanol solutions (on the average between 70 and 90 s), the EOF
333 remained somewhat similar in aqueous and methanol based background electrolytes, but slowed

334 down significantly in ethanol based background electrolytes (Figure 4C). Depending on the
335 background electrolyte, the linear flow rates varied within 0.2-1 mm/s corresponding to volume flow
336 rates between 30 and 150 nL/min. At the same time, the electrophoretic mobilities were differently
337 affected (due to the ϵ/η ratio), which eventually resulted in better resolving power ($R_s=0.9$) in
338 acidified ethanol than in aqueous or methanol based electrolytes (Figures 4A and B). The absolute
339 migration time repeatability was generally better in aqueous conditions (Figure 4C), whereas non-
340 aqueous electrolytes clearly increased the ionization efficiency (Figure 4D) and improved the plate
341 heights (Figure 4E). On the average, the peak areas increased 2-fold in ethanol-based electrolytes
342 compared to those in aqueous electrolytes and showed sufficiently good repeatability from run to run
343 (6.6% and 16.2% RSD for Ang I and Ang II, $n=6$, with Ang III as the internal standard). The
344 theoretical plate numbers also increased 2-fold, to $1.2 \times 10^4 \text{ m}^{-1}$ (Ang I) and $2.4 \times 10^4 \text{ m}^{-1}$ (Ang II), in
345 ethanol-based electrolytes.

346

347 In general, the ability to carry out microchip-NACE-ESI-MS with overall performance similar to or
348 better than those obtained in aqueous conditions broadens out the applicability of thiol-ene
349 microdevices to encompass a variety of bioanalytical purposes. Even if NACE is commonly used in
350 the analyses of water-insoluble or sparingly soluble analytes, it may also provide improved resolution
351 of the separation of water-soluble, charged analytes, because of the differences between the
352 electrophoretic mobilities in non-aqueous and aqueous electrolytes. In addition to this work, increased
353 resolving power in peptide separation by NACE has also been reported elsewhere. [38-41] In general,
354 microchip NACE is also a good fit to ESI-MS due to the similarity of the flow rates and the solvents
355 required. The low surface tension of organic background electrolytes improves and stabilizes the
356 electrospray and thus increases the ionization efficiency over those of aqueous background
357 electrolytes. On the other hand, the possibility to perform separations in either aqueous or non-
358 aqueous conditions by using the same chip, provides greater practical flexibility in analytical method

359 development and has potential for improving resolution between compounds that do not sufficiently
360 resolve in aqueous conditions, such as angiotensins I and II. Thiol-enes as chip fabrication materials
361 play a key role in facilitating the analyses in organic solvents without degradation and thus, leaching
362 of the monomer residues to the MS.

363

364 **4. CONCLUSIONS**

365 The inherent good solvent compatibility of thiol-enes was exploited to carry out microchip
366 electrophoresis in non-aqueous conditions in addition to more commonly applied aqueous
367 background electrolytes. We found that NACE-ESI-MS improved particularly the sensitivity and
368 selectivity of angiotensin peptides over MCE-ESI-MS in aqueous conditions. In addition, the replica-
369 molding of thiol-enes was shown to be a versatile tool for low-cost fabrication of MCE chips with
370 integrated sharp-pointed ESI emitters. The fabrication process proceeds from a single lithographically
371 fabricated SU-8 master but after that, numerous microfluidic chips can be fabricated using replica
372 molding and bonding techniques under standard laboratory conditions. The materials' properties and
373 the surface chemistry of the thiol-ene chips can be tuned simply by changing the precursor chemicals
374 or adjusting the stoichiometry of the monomers. The material stability and the electrospray
375 experimental data suggest that both stoichiometric and off-stoichiometric thiol-ene compositions
376 (from 50 mol-% excess of allyls to 50 mol-% excess of tetrathiols) are feasible for the replication of
377 sharp emitter tips. High quality spectra with negligible background interference were obtained when
378 using the stoichiometric composition. However, off-stoichiometric thiol-ene compositions resulted in
379 the leaching of the excess monomer into the MS, but the monomer background could be easily
380 eliminated by carefully rinsing the channels prior to use. The results suggest that replica-molding of
381 thiol-enes provides a simple, low-cost and flexible approach to the fabrication of microchips under
382 standard laboratory conditions, which significantly promotes the adaptation of the microchip
383 technology for routine analyses.

384 **ACKNOWLEDGEMENTS**

385 The research that led to these results received funding from the European Research Council (ERC)
386 under the European Union's Seventh Framework Programme (FP/2007-2013) / ERC Grant
387 Agreement number 311705 (CUMTAS). The work was also financially supported by the Academy
388 of Finland (grant number 266820), the University of Helsinki Research Funds, and the CHEMS
389 doctoral programme, University of Helsinki. We thank the Electron Microscopy Unit of the Institute
390 of Biotechnology, University of Helsinki, for providing access to the scanning electron microscope,
391 and the Micronova Nanofabrication Centre, Aalto University, for providing access to the cleanroom
392 facilities.

393

394 **APPENDIX A. Supplementary data**

395 Supplementary data associated with this article can be found, in the online version.

396

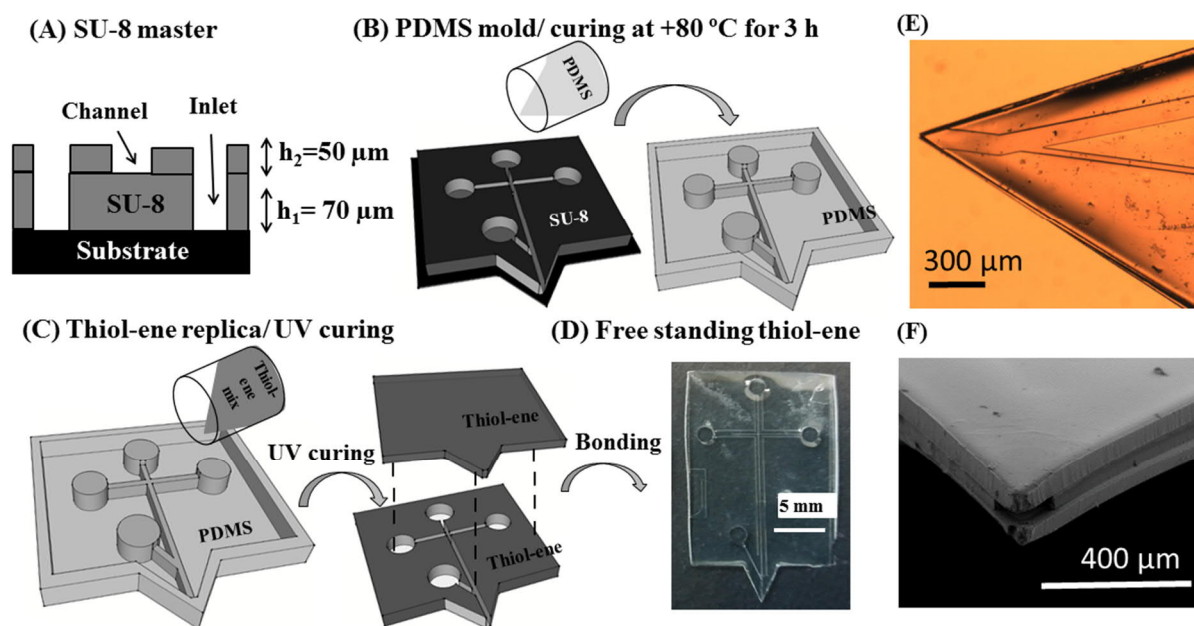
397 **REFERENCES**

- 398 [1] D. Gao, H. Liu, Y. Jiang, J. Lin, Recent advances in microfluidics combined with mass
399 spectrometry: technologies and applications, *Lab Chip* 13 (2013) 3309-3322.
- 400 [2] T. Sikanen, S. Franssila, T.J. Kauppila, R. Kostiainen, T. Kotiaho, R.A. Ketola, Microchip
401 technology in mass spectrometry, *Mass Spectrom. Rev.* 29 (2010) 351-391.
- 402 [3] S. Koster, E. Verpoorte, A decade of microfluidic analysis coupled with electrospray mass
403 spectrometry: An overview, *Lab Chip* 7 (2007) 1394-1412.
- 404 [4] P. Hoffmann, M. Eschner, S. Fritzsche, D. Belder, Spray performance of microfluidic glass
405 devices with integrated pulled nanoelectrospray emitters, *Anal. Chem.* 81 (2009) 7256-7261.
- 406 [5] J. Mellors, V. Gorbounov, R. Ramsey, J. Ramsey, Fully integrated glass microfluidic device for
407 performing high-efficiency capillary electrophoresis and electrospray ionization mass spectrometry,
408 *Anal. Chem.* 80 (2008) 6881-6887.
- 409 [6] A.G. Chambers, J.M. Ramsey, Microfluidic dual emitter electrospray ionization source for
410 accurate mass measurements, *Anal. Chem.* 84 (2012) 1446-1451.
- 411 [7] L. Sainiemi, T. Sikanen, R. Kostiainen, Integration of fully microfabricated, three-dimensionally
412 sharp electrospray ionization tips with microfluidic glass chips, *Anal. Chem.* 84 (2012) 8973-8979.

- 413 [8] E. Mery, F. Ricoul, N. Sarrut, O. Constantin, G. Delapierre, J. Garin, F. Vinet, A silicon
414 microfluidic chip integrating an ordered micropillar array separation column and a nano-
415 electrospray emitter for LC/MS analysis of peptides, *Sens. Actuators B: Chem.* 134 (2008) 438-446.
- 416 [9] L. Sainiemi, T. Nissilä, R. Kostiainen, S. Franssila, R.A. Ketola, A microfabricated micropillar
417 liquid chromatographic chip monolithically integrated with an electrospray ionization tip, *Lab Chip*
418 12 (2012) 325-332.
- 419 [10] T. Sikanen, S. Tuomikoski, R.A. Ketola, R. Kostiainen, S. Franssila, T. Kotiaho, Fully
420 microfabricated and integrated SU-8-based capillary electrophoresis-electrospray ionization
421 microchips for mass spectrometry, *Anal. Chem.* 79 (2007) 9135-9144.
- 422 [11] T. Sikanen, S. Aura, S. Franssila, T. Kotiaho, R. Kostiainen, Microchip capillary
423 electrophoresis–electrospray ionization–mass spectrometry of intact proteins using uncoated
424 Ormocomp microchips, *Anal. Chim. Acta* 711 (2012) 69-76.
- 425 [12] J. Wen, Y. Lin, F. Xiang, D.W. Matson, H.R. Udseth, R.D. Smith, Microfabricated isoelectric
426 focusing device for direct electrospray ionization-mass spectrometry, *Electrophoresis* 21 (2000)
427 191-197.
- 428 [13] H. Shinohara, T. Suzuki, F. Kitagawa, J. Mizuno, K. Otsuka, S. Shoji, Polymer microchip
429 integrated with nano-electrospray tip for electrophoresis–mass spectrometry, *Sens. Actuators B:*
430 *Chem.* 132 (2008) 368-373.
- 431 [14] S. Thorslund, P. Lindberg, P.E. Andréén, F. Nikolajeff, J. Bergquist, Electrokinetic-driven
432 microfluidic system in poly (dimethylsiloxane) for mass spectrometry detection integrating sample
433 injection, capillary electrophoresis, and electrospray emitter on-chip, *Electrophoresis* 26 (2005)
434 4674-4683.
- 435 [15] X. Sun, R.T. Kelly, K. Tang, R.D. Smith, Ultrasensitive nanoelectrospray ionization-mass
436 spectrometry using poly (dimethylsiloxane) microchips with monolithically integrated emitters,
437 *Analyst* 135 (2010) 2296-2302.
- 438 [16] K. Huikko, P. Östman, K. Grigoras, S. Tuomikoski, V. Tiainen, A. Soinen, K. Puolanne, A.
439 Manz, S. Franssila, R. Kostiainen, Poly (dimethylsiloxane) electrospray devices fabricated with
440 diamond-like carbon–poly (dimethylsiloxane) coated SU-8 masters, *Lab Chip* 3 (2003) 67-72.
- 441 [17] R. Gomez-Sjoberg, A.A. Leyrat, B.T. Houseman, K. Shokat, S.R. Quake, Biocompatibility and
442 Reduced Drug Absorption of Sol–Gel-Treated Poly (dimethyl siloxane) for Microfluidic Cell
443 Culture Applications, *Anal. Chem.* 82 (2010) 8954-8960.
- 444 [18] B.T. Good, S. Reddy, R.H. Davis, C.N. Bowman, Tailorable low modulus, reversibly
445 deformable elastomeric thiol–ene materials for microfluidic applications, *Sens. Actuators B: Chem.*
446 120 (2007) 473-480.
- 447 [19] S.M. Tähkä, A. Bonabi, M. Nordberg, M. Kanerva, V.P. Jokinen, T.M. Sikanen, Thiol-ene
448 microfluidic devices for microchip electrophoresis: Effects of curing conditions and monomer
449 composition on surface properties, *J. Chromatogr. A* 1426 (2015) 233-240.

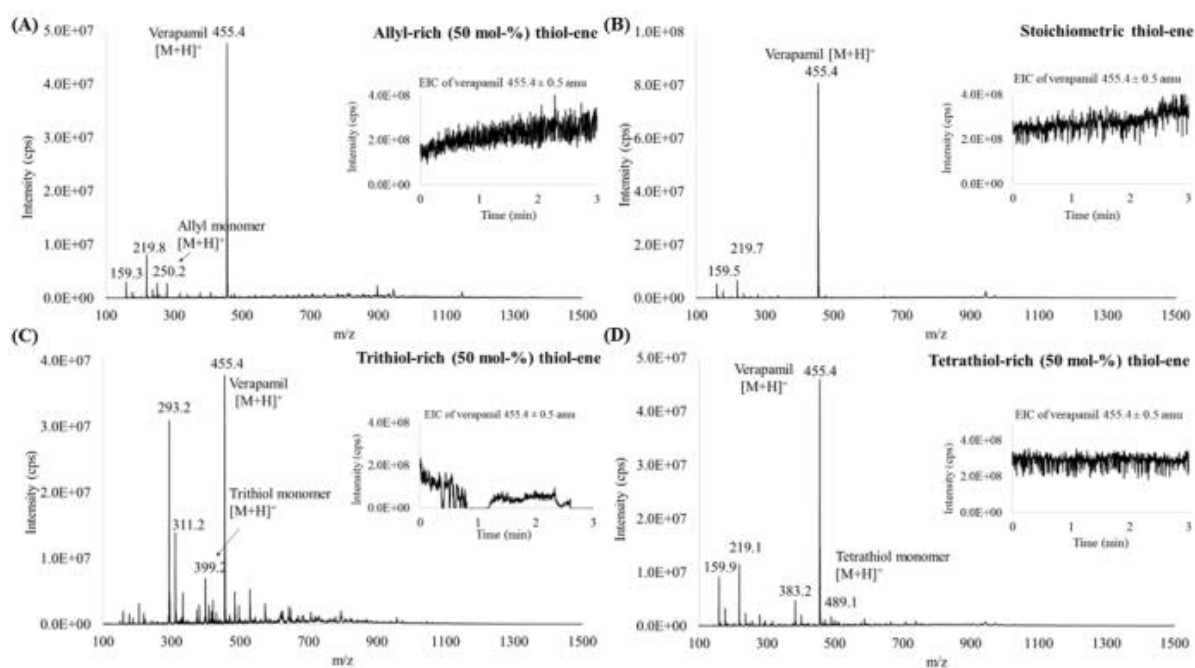
- 450 [20] V.S. Khire, Y. Yi, N.A. Clark, C.N. Bowman, Formation and Surface Modification of
451 Nanopatterned Thiol-ene Substrates using Step and Flash Imprint Lithography, *Adv Mater* 20
452 (2008) 3308-3313.
- 453 [21] C.F. Carlborg, T. Haraldsson, K. Öberg, M. Malkoch, W. van der Wijngaart, Beyond PDMS:
454 off-stoichiometry thiol-ene (OSTE) based soft lithography for rapid prototyping of microfluidic
455 devices, *Lab Chip* 11 (2011) 3136-3147.
- 456 [22] K. Mesbah, T.D. Mai, T.G. Jensen, L. Sola, M. Chiari, J.P. Kutter, M. Taverna, A neutral
457 polyacrylate copolymer coating for surface modification of thiol-ene microchannels for improved
458 performance of protein separation by microchip electrophoresis, *Microchim. Acta*(2016) 1-11.
- 459 [23] J.P. Lafleur, S. Senkbeil, J. Novotny, G. Nys, N. Bøgelund, K.D. Rand, F. Foret, J.P. Kutter,
460 Rapid and simple preparation of thiol-ene emulsion-templated monoliths and their application as
461 enzymatic microreactors, *Lab Chip*(2015) .
- 462 [24] J.P. Lafleur, R. Kwapiszewski, T.G. Jensen, J.P. Kutter, Rapid photochemical surface
463 patterning of proteins in thiol-ene based microfluidic devices, *Analyst* 138 (2013) 845-849.
- 464 [25] N.A. Feidenhans'l, J.P. Lafleur, T.G. Jensen, J.P. Kutter, Surface functionalized thiol-ene
465 waveguides for fluorescence biosensing in microfluidic devices, *Electrophoresis* 35 (2014) 282-288.
- 466 [26] T.M. Sikanen, J.P. Lafleur, M. Moilanen, G. Zhuang, T.G. Jensen, J.P. Kutter, Fabrication and
467 bonding of thiol-ene-based microfluidic devices, *J Micromech. Microeng* 23 (2013) 037002.
- 468 [27] L.R. Gibson 2nd, P.W. Bohn, Non-aqueous microchip electrophoresis for characterization of
469 lipid biomarkers, *Interface Focus.* 3 (2013) 20120096.
- 470 [28] M.L. Cable, A.M. Stockton, M.F. Mora, P.A. Willis, Low-temperature microchip nonaqueous
471 capillary electrophoresis of aliphatic primary amines: applications to Titan chemistry, *Anal. Chem.*
472 85 (2012) 1124-1131.
- 473 [29] H. Hu, X. Yin, X. Wang, H. Shen, A study on the system of nonaqueous microchip
474 electrophoresis with on-line peroxyoxalate chemiluminescence detection, *J. Sep. Sci* 36 (2013) 713-
475 720.
- 476 [30] N. Nuchtavorn, P. Smejkal, M.C. Breadmore, R.M. Guijt, P. Doble, F. Bek, F. Foret, L.
477 Suntornsuk, M. Macka, Exploring chip-capillary electrophoresis-laser-induced fluorescence field-
478 deployable platform flexibility: Separations of fluorescent dyes by chip-based non-aqueous
479 capillary electrophoresis, *J. Chromatogr. A* 1286 (2013) 216-221.
- 480 [31] T. Wu, Y. Mei, J.T. Cabral, C. Xu, K.L. Beers, A new synthetic method for controlled
481 polymerization using a microfluidic system, *J. Am. Chem. Soc.* 126 (2004) 9880-9881.
- 482 [32] Z.T. Cygan, J.T. Cabral, K.L. Beers, E.J. Amis, Microfluidic platform for the generation of
483 organic-phase microreactors, *Langmuir* 21 (2005) 3629-3634.
- 484 [33] C. Harrison, J.T. Cabral, C.M. Stafford, A. Karim, E.J. Amis, A rapid prototyping technique
485 for the fabrication of solvent-resistant structures, *J Micromech Microeng.* 14 (2004) 153.

- 486 [34] A.P. Dahlin, M. Wetterhall, G. Liljegren, S.K. Bergström, P. André, L. Nyholm, K.E.
487 Markides, J. Bergquist, Capillary electrophoresis coupled to mass spectrometry from a polymer
488 modified poly (dimethylsiloxane) microchip with an integrated graphite electrospray tip, *Analyst*
489 130 (2005) 193-199.
- 490 [35] K. Faserl, B. Sarg, L. Kremser, H. Lindner, Optimization and Evaluation of a Sheathless
491 Capillary Electrophoresis–Electrospray Ionization Mass Spectrometry Platform for Peptide
492 Analysis: Comparison to Liquid Chromatography–Electrospray Ionization Mass Spectrometry,
493 *Anal. Chem.* 83 (2011) 7297-7305.
- 494 [36] GenScript Peptide Property Calculator, 2014 .
- 495 [37] N. Nordman, S. Laurén, T. Kotiaho, S. Franssila, R. Kostianen, T. Sikanen, Interfacing
496 microchip isoelectric focusing with on-chip electrospray ionization mass spectrometry, *J.*
497 *Chromatogr. A* 1398 (2015) 121-126.
- 498 [38] A. Psurek, C. NEUSÜSS, M. Pelzing, G.K. Scriba, Analysis of the lipophilic peptaibol
499 alamethicin by nonaqueous capillary electrophoresis-electrospray ionization-mass spectrometry,
500 *Electrophoresis* 26 (2005) 4368-4378.
- 501 [39] A. Psurek, F. Matysik, G.K. Scriba, Determination of enkephalin peptides by nonaqueous
502 capillary electrophoresis with electrochemical detection, *Electrophoresis* 27 (2006) 1199-1208.
- 503 [40] A. Psurek, S. Feuerstein, D. Willbold, G.K. Scriba, Nonaqueous versus aqueous capillary
504 electrophoresis of α -helical polypeptides: Effect of secondary structure on separation selectivity,
505 *Electrophoresis* 27 (2006) 1768-1775.
- 506 [41] A. Psurek, G.K. Scriba, Peptide separations and dissociation constants in nonaqueous capillary
507 electrophoresis: Comparison of methanol and aqueous buffers, *Electrophoresis* 24 (2003) 765-773.



509

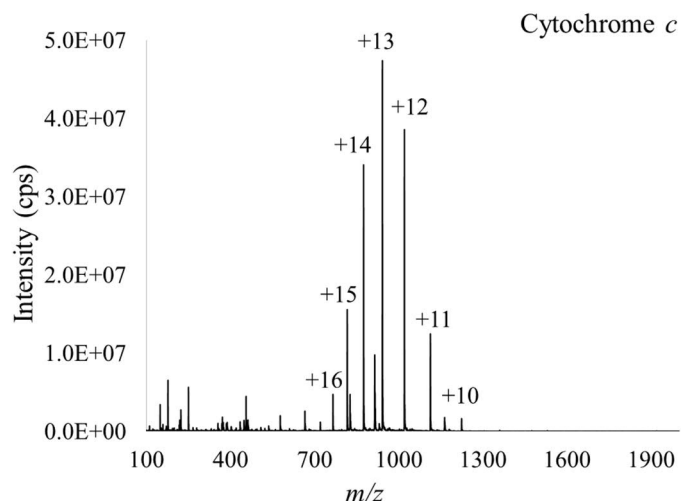
510 **Figure 1.** (A-D) Schematic presentation of the fabrication steps of thiol-ene MCE-ESI-chips (not in
 511 scale): (A) SU-8 master fabrication in cleanroom by spincoating two sequential layers of SU-8 over
 512 silicon substrate ($h_1=70\ \mu\text{m}$ inlets and $h_2=50\ \mu\text{m}$ channels), (B) casting of the PDMS mold and
 513 curing by heat, (C) replication and UV curing of the thiol-ene top and bottom layers followed by tip
 514 alignment and bonding, (D) photograph of a bonded free-standing thiol-ene chip. (E-F) Optical and
 515 scanning electron micrographs of an ESI emitter tip after bonding.



516

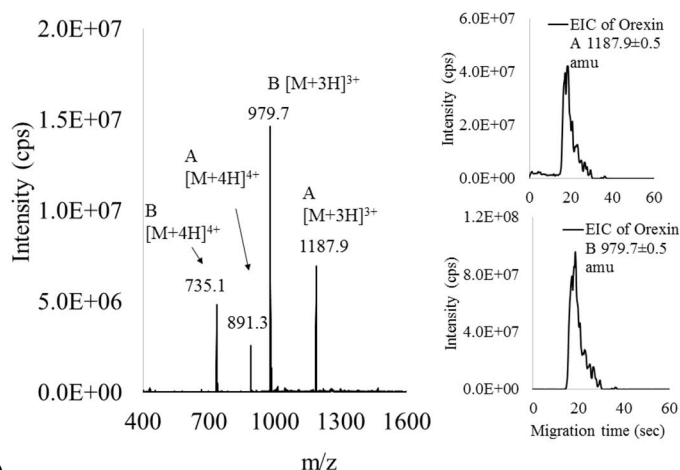
517 **Figure 2.** ESI-MS spectra obtained by direct infusion from thiol-ene chips that had been fabricated
 518 from (A) allyl-rich (50 mol-%), (B) stoichiometric, (C) thiol-rich (50 mol-%, trithiol) and (D) thiol-
 519 rich (50 mol-%, tetrathiol) compositions. The curing times used were 10 min in each. The sample
 520 solution was 5 μ M verapamil in methanol-water 80:20 containing 1% acetic acid. The ESI voltage
 521 applied was 3kV.

522



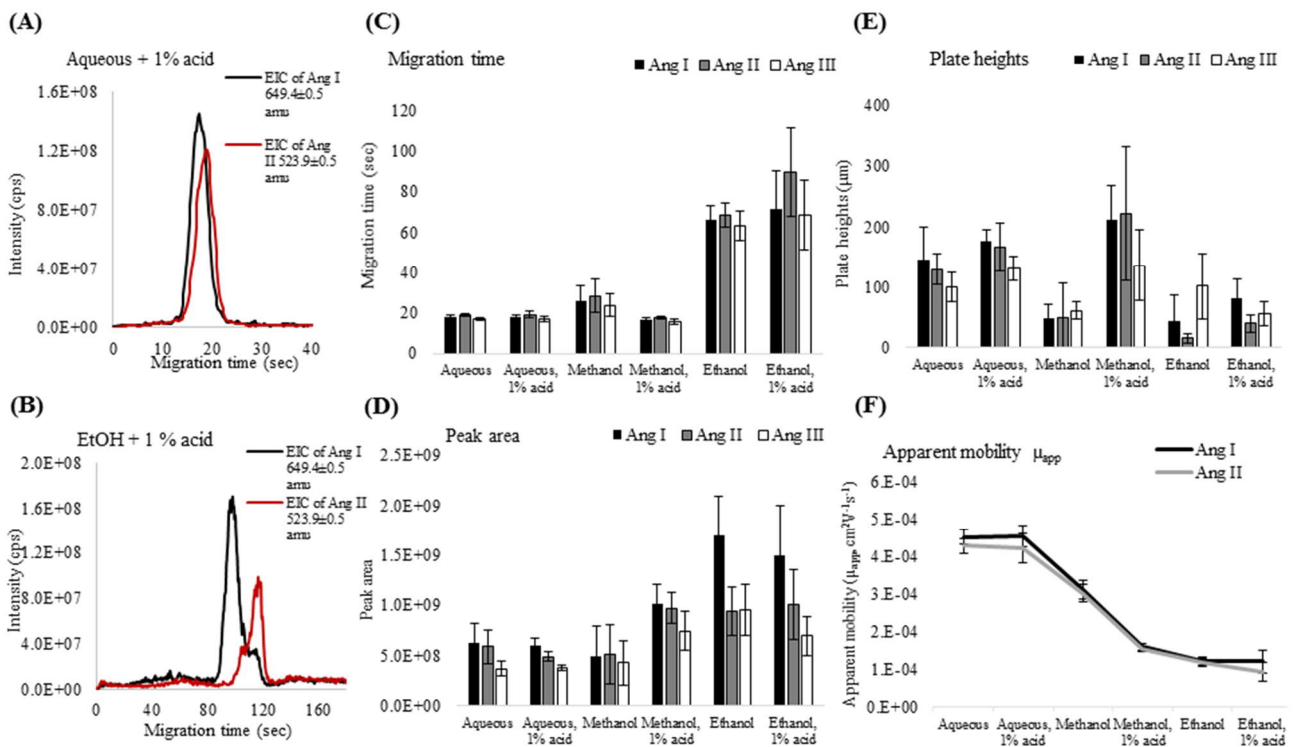
523 A)

Neuropeptides orexin A and B



524 B)

525 **Figure 3.** (A) The direct infusion mass spectrum of 5 $\mu\text{g/mL}$ cytochrome *c* in 20 mM ammonium
 526 acetate containing 50% methanol was obtained by using the allyl-rich chip and electric field
 527 strength of 750 V cm^{-1} (between the BI and the MLI). (B) The mass spectra and extracted ion
 528 electropherograms of orexin A (356 $\mu\text{g/mL}$) and orexin B (294 $\mu\text{g/mL}$) injected for 20.0 s and
 529 separated in 20 mM ammonium acetate containing 40 % methanol. The analysis was carried out by
 530 using the stoichiometric chip and electric field strength of 500 V cm^{-1} . (B) In both analyses, makeup
 531 liquid was methanol–water 80:20 containing 1% acetic acid and the ESI voltage was 3.5 kV



532

533 **Figure 4.** (A-B) Extracted ion chromatograms of angiotensin peptides (each 100 $\mu\text{g/mL}$) in 20 mM
 534 ammonium acetate containing 40% methanol and 1% (v/v) acetic acid (A) and in 20 mM
 535 ammonium acetate in ethanol containing 1% (v/v) acetic acid (B). (C-F) Comparison of the aqueous
 536 and non-aqueous MCE-ESI-MS analyses by means of migration time (C), peak area (D), plate
 537 heights (E) and apparent mobility (F). The aqueous electrolyte used was 20 mM ammonium acetate
 538 containing 40 % methanol with or without 1% (v/v) acetic acid. The non-aqueous electrolytes used
 539 contained either 10 mM (methanol) or 20 mM (ethanol) ammonium acetate in pure organic solvent,
 540 with or without 1% (v/v) acetic acid. The apparent pH ranges of the BGEs were 4.5-6.4 (with acid)
 541 and 7.1-8.1 (without acid). In all runs, the electric field strength was 250 Vcm^{-1} with ESI voltage of
 542 3.5 kV and the makeup liquid was methanol-water 80:20 containing 1 % (v/v) acetic acid. The error
 543 bars (C-F) represent the standard deviations of n=4-5 repeated runs.